Journal Pre-proofs

Volumetric internal Joule heating of a catalyst packed SiSiC foam for efficient dry reforming of methane

Lei Zheng, Di Wang, Yunfeng Jiang, Yingyu Ren, Yihai Wu, Yu Fu, Jun Zhang

PII: S1385-8947(24)09782-1
DOI: https://doi.org/10.1016/j.cej.2024.158291
Reference: CEJ 158291

To appear in: *Chemical Engineering Journal*

Received Date: 28 October 2024
Revised Date: 24 November 2024
Accepted Date: 3 December 2024

Please cite this article as: L. Zheng, D. Wang, Y. Jiang, Y. Ren, Y. Wu, Y. Fu, J. Zhang, Volumetric internal Joule heating of a catalyst packed SiSiC foam for efficient dry reforming of methane, *Chemical Engineering Journal* (2024), doi: https://doi.org/10.1016/j.cej.2024.158291

Volumetric internal Joule heating of a catalyst packed SiSiC foam for efficient dry reforming of methanes

Lei Zheng [1,*], Di Wang [1], Yunfeng Jiang [1,2], Yingyu Ren [1], Yihai Wu [3], Yu Fu [1], Jun Zhang [1,*]

[1] CAS Key Laboratory of Low-Carbon Conversion Science and Engineering, Shanghai Advanced Research Institute, Chinese Academy of Sciences, Shanghai 201210, P.R. China

[2] University of Chinese Academy of Sciences, Beijing 100049, P.R. China

[3] Gaolu Air Products and Chemicals (Shanghai) Energy Technology Co., Ltd, Shanghai 201620, P. R. China

* Corresponding authors: zhengl@sari.ac.cn (L. Zheng); zhangj@sari.ac.cn (J. Zhang)

Highlights:

- Direct internal Joule heating of a catalyst packed SiSiC foam configuration;
- Selective Joule heating is energy saving and ensures low reactor wall T;
- SiSiC foam provides volumetric heating with uniform T distribution;
- Internal Joule heating ensures higher DRM activity than external heating.

Abstract:

The strong endothermic dry reforming of methane (DRM) is a reaction of interest to convert greenhouse gases into syngas for downstream chemical synthesis. However, conventional external combustion heating not only generates unwanted CO_2 emissions but also suffers from heat transfer limitations. With the rising trend of renewable electricity, process electrification with Joule heating emerges as a promising alternative to combustion, facilitating decarbonization and process intensification. In this study, we systematically assessed the catalytic performance in direct Joule heating of an internal SiSiC open-cell foam packed with Ni-based pellet catalysts for DRM reaction. The interconnected porous structure of SiSiC foam enables selective and volumetric heating of pellet catalysts in a packed bed configuration. The direct selective heating of internal structure requires extremely low input power, *i.e.*, only 65 W to reach 800 °C compared to 143 W for external oven heating, and results in a reactor wall temperature approx. 300 °C lower than from the foam centerline, with the potential to significantly reduce reactor material requirements and cost. Additionally, volumetric Joule heating provides more uniform heating profiles and approx. 30 °C higher average temperatures over the catalytic bed with no cold spots observed, leading to enhanced methane and CO_2 conversions reaching 94% and 64% at 800 °C, respectively, which are approx. 5-10% higher than external heating at the same foam outlet temperatures. The Joule-heated DRM ensures a significantly low specific energy demand of approx. 0.71 kWh/Nm³ for syngas production. The insights gained from this work are in principle transferable to direct Joule heating of internal structured catalysts for other endothermic reactions.

Keywords:

Joule heating; Dry reforming of methane; Internal structures; Selective heating; Volumetric heating

TOC Figure:

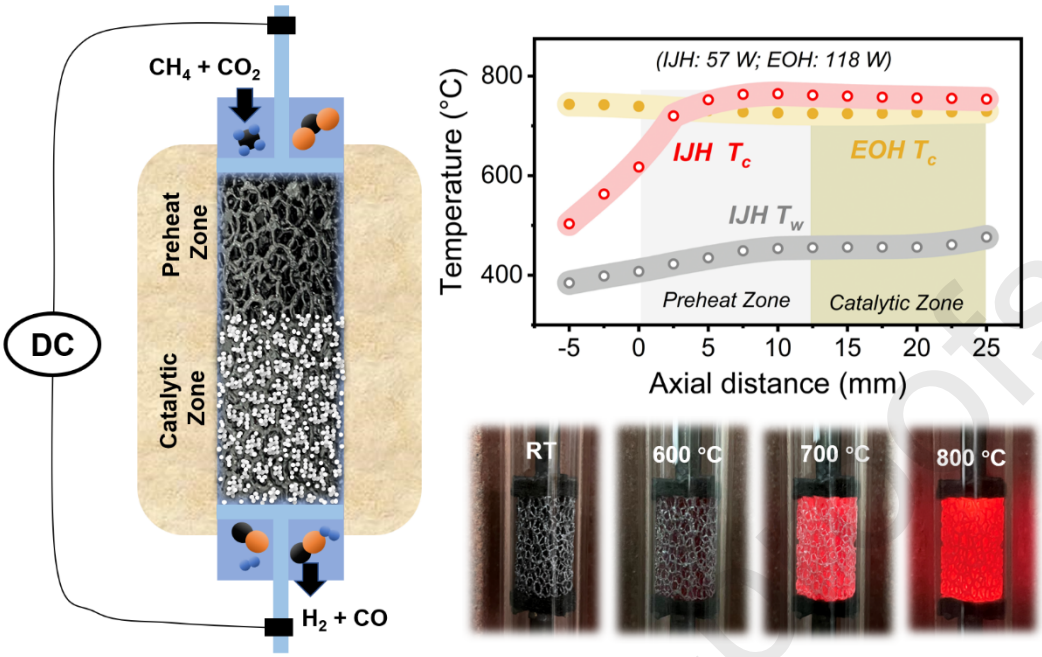

1. Introduction

Advanced decarbonization solutions are urgently required for the energy-intensive chemical industry as a result of growing environmental concerns. Dry reforming of methane (DRM) [1-4], which converts methane and captured CO_2 into syngas for the downstream synthesis of chemicals and fuels, offers an attractive approach to mitigate CO_2 emissions and presents as an important opportunity to meet the growing demand for energy and chemicals through a more sustainable pathway. Dry reforming of methane is of great interest but remains very challenging as the highly endothermic nature, which necessitates substantial energy input for high temperature operation to achieve sufficient high conversions [1]. The conventional fuel combustion process used to supply the necessary reaction heat results in unwanted CO_2 emissions, undermining decarbonization efforts [5, 6]. On the other hand, the conventional fuel combustion process where heat is typically generated outside the reactor results in limited heat transfer rates. This may induce temperature gradients within the reactor and potentially lead to side reactions and catalyst deactivation associated with sintering and coking [2].

With the increasing availability of low-cost renewable electricity, high-temperature chemical processes that rely on combustion heat can be replaced with decarbonized heat from green electricity, *i.e.*, process electrification, ushering the chemical industry into a new electric decade [6-8]. Joule heating, induction heating, microwave heating and thermal plasma are the state-of-the-art power-to-heat methods for process electrification [9-12]. Among them, Joule heating, also known as resistive heating or ohmic heating, has recently been extensively exploited to promote endothermic reactions toward decarbonization and process intensification [13-20]. Recent studies show that electrified dry reforming of methane (eDRM) based on Joule heating exhibited low energy demand for CO_2 conversion [5], and the rapid pulse Joule heating with extremely short high temperature durations enables catalyst regeneration with *in-situ* coke removal [17]. Moreover, several process simulations studies have demonstrated that electrified methane reforming processes using Joule heating with renewable electricity is a promising route from energy, environmental and economic perspective [21-24].

Driven by a specific heating principle, it is essential to design the Joule-heated reactor through careful selection of the appropriate material and geometry for the heating elements, with innovative technical solutions and appropriate infrastructure to maximize energy efficiency [9, 20]. The Joule heating substrates should be conductive and continuous materials, capable to be heated up to reasonable high temperatures while remaining stable under

reaction conditions. Direct Joule heating of pellet catalysts presents challenges primarily due to the inherent complexities associated with controlling the contact area [19, 25]. Chorkendorff and coworkers reported the electrified reactor concept that utilizes direct Joule heating of the reactor wall made of FeCrAl alloy [13]. The catalyst was inner coated on the heating element, and a low thermal gradient of less than 2 °C across the washcoat was reported, the excellent heat transfer properties ensure outstanding catalytic performance [26]. However, such reactor concept is controlled by mass transfer limitations [27], and electrically conductive honeycombs may provide a viable method for scaling up the electrified wall reactor concept, as demonstrated in the pilot plant study conducted by Mortensen and coworkers [28]. In addition to above mentioned electrified catalyst and electrified reactor concepts, most studies focus on the direct heating of elements within the reactor, utilizing various structures such as wires [18, 29, 30], plates [16, 17, 31], honeycomb monolith and open-cell foams [5, 14, 32-37]. Typically, the catalysts can either be coated on the heating substrates or incorporated as pellet catalysts packed within the voids of the heating elements. In view of process intensification, optimizing mass transfer properties in Joule-heated reactors is as critical as enhancing heat transfer. Compared to other structures which may processed with limited surface areas and suboptimal gas-solid mass transfer, open-cell foams feature a porous structure which induces tortuous flow [38], and can significantly improving mass transfer efficiency [5, 14, 32-34, 39].

In previous works, the direct Joule heating of the SiSiC open-cell foam with washcoated Rh/Al_2O_3 catalyst was studied for different endothermic reactions [5, 14, 32], demonstrating excellent catalytic performances. The configuration of catalyst washcoated on heating elements ensures excellent heat transfer but may suffer from possible mechanical strength issues, particularly at high space velocities. Furthermore, a systematic analysis of the temperature distribution in the Joule-heated catalytic bed is essential to highlight the advantages of Joule heating, such as selective and uniform heating. In this work, we extended such concept by utilizing SiSiC foam as an internal Joule heating substrate with non-noble metal Ni-based pellet catalysts in a packed bed configuration for dry reforming of methane. We have systematically evaluated the heating properties and temperature distribution in the direct internal Joule-heated process, and compared to the results from conventional external oven heating. In general, the internal Joule heating provides more selective and uniform heat distribution than external method, resulting in a more energy-efficient dry reforming of methane process with improved methane and CO_2 conversions under the same reaction conditions.

2. Materials and methods

2.1 SiSiC open-cell foam characterization

In this work, a commercial cylindrical Si-infiltrated silicon carbide (SiSiC) open-cell foam (OD = 15 mm, L = 25 mm, 25 PPI) was adopted as internal Joule heating substrate. The foam has a cylindrical hole (ID = 3 mm) in the center in order to place thermocouple for temperature distribution measurement. The foam geometry was characterized by operating a Hitachi S-4800 scanning electron microscope (SEM) at 3 kV. The pore diameter (d_p) and the strut diameter (d_s) were obtained by averaging more than 50 measurements from the obtained SEM images using an open-source software (ImageJ2x). X-ray diffraction (XRD) pattern of the SiSiC foam was recorded using a Rigaku Ultima IV powder diffractometer with Cu Kα radiation as a source of radiation (λ = 0.15408 nm) at 40 kV and 40 mA, in the range of 2θ = 20°-70°, a step size of 0.05° and a step time of 12.5 s. Ethanol picnometry method was adopted to evaluate the total porosity of the foam.

2.2 Catalyst preparation and characterization

The 10% Ni/Al_2O_3 catalyst was prepared in the present work by a wetness impregnation method, using nickel (II) nitrate hexahydrate ($Ni(NO_3)_2 \cdot 6H_2O$, Sigma-Aldrich) as Ni precursor. A commercial γ-Al_2O_3 support (General-Reagent) was used and calcined in static air at 800 °C for 4 h prior to impregnation. Homemade deionized water (18.5 MΩ·cm) was used for the catalyst preparation. In a typical process, the target amount of Ni precursor was dissolved in water and the obtained precursor solution was mixed with γ-Al_2O_3. The powders were dried in oven at 120 °C overnight, followed with calcination at 800 °C for 4 h in a muffle oven with a temperature ramp of 10° C/min.

Similar to the foam characterization, the morphology of the prepared Ni/Al_2O_3 catalyst was characterized with the Hitachi S-4800 scanning electron microscope (SEM) at 3 kV, and the XRD pattens of Al_2O_3 support and Ni/Al_2O_3 catalyst were recorded on same diffractometer with a different 2θ range of 10°-90°. N_2-physical adsorption-desorption experiments were carried out on a Micromeritics ASAP 2420 physisorption analyzer. Prior to the measurement, all samples were degassed in vacuum at 300 °C for 10 h. The adsorption-desorption tests were conducted at -196 °C, and the specific surface area (S_{BET}) of the samples was calculated using the Brunauer-Emmett-Teller (BET) method. X-ray photoelectron spectroscopy (XPS) was conducted using a Thermo Fisher Scientific ESCALAB 250Xi analyzer, utilizing Al Kα radiation as the radiation source (hv = 1486.76 eV). The

pressure within the sample chamber was maintained below 8.6×10^{-7} Torr. The calibration of binding energy values for all samples was performed using a C 1s peak at 284.8 eV. X-ray absorption spectroscopy (XAS) of the Ni/Al_2O_3 catalyst at Ni K-edge were performed at the BL11B beamline of the Shanghai Synchrotron Radiation Facility (SSRF). X-ray absorption spectra of the samples were recorded in transmission mode. In addition to Ni/Al_2O_3 catalyst, two reference samples, *i.e.*, Ni foil and NiO were also measured for comparison. The XAS spectra obtained were normalized using the ATHENA program.

2.3 Catalytic activity tests

All catalytic performance tests were carried out at steady-state condition in a quartz tube reactor (ID = 17 mm). The quartz tube reactor was positioned inside an electric oven, allowing for oven heating of the reactor from outside. In addition to conventional oven heating, the reactor was also designed for direct Joule heating, which will be explained in the following. Gases were dosed individually by mass flow controllers (Sevenstar) and mixed before entering the quartz reactor. The gas composition after the reactor was analyzed with a micro-GC (Fanwei FV3320). Water was removed from the products before entering the GC for analysis. The inert gas (nitrogen) was directly fed to the analysis section through a by-pass line (without passing through reactor) to enable the use of internal standard for GC analysis.

For the catalytic tests, 100 mg of Ni/Al_2O_3 catalyst (40-60 mesh) was mixed with 3 g of quartz sand (40-60 mesh, General-Reagent), and the resulting mixture was placed in the voids of SiSiC foam, filling half of the foam voids, with the unpacked portion serving as a preheating zone. A thin layer of quartz wool was placed between the SiSiC foam and the quartz reactor tube. Two layers of porous carbon fiber, thickness of 3 mm, were placed on the top and bottom sides of the foam to ensure good contact with the electrodes. These electrodes were connected to an adjustable DC power supply (A-BF SS-2050KDS, V_{max} = 20 V, I_{max} = 50 A) for Joule heating of the SiSiC foam. In order to ensure optimal contact between the SiSiC foam and electrodes, and to compensate the thermal expansion of SiSiC foam, a durable metallic frame structure was employed to fix the electrodes. For each Joule heating test, the target temperature was achieved by adjusting the input electric voltage, and the output current will be self-adjusted according to the electric resistance of the heating system.

Several K-type thermocouples were strategically positioned in the catalytic reactor to monitor the temperatures. A sliding thermocouple (T_c), electrically insulated by a quartz tube (OD = 3 mm; ID = 2 mm), was inserted into the

inner cylindrical hole of the SiSiC foam via the upstream electrode, enables the temperature distribution measurement within the foam. Temperatures were measured with a resolution of 5 mm over a total length of 30 mm from the bottom of the foam. Another sliding thermocouple (T_w) was positioned at the outer wall of the reactor tube to assess the wall temperature distribution. The temperature after the foam outlet (T_{down}) was measured using a fixed thermocouple, also insulated by a quartz tube, located within the downstream electrode. Additionally, the temperature of the electric oven (T_{oven}) was monitored by a dedicated thermocouple for precise temperature control for tests in EOH mode.

In order to demonstrate the advantage of direct internal Joule heating, we have carried out the Joule heating in two configurations with and without thermal insulation: (i) internal Joule heating with oven door closed (IJH-DC) and (ii) internal Joule heating with oven door open (IJH-DO). The results were then compared to those obtained from (iii) conventional external oven heating (EOH). Prior to the catalytic tests, the loaded catalysts were reduced under 100 mL/min flow of H_2/N_2 (1/1) by heating from room temperature to 800 °C with a temperature ramp of 10°C/min and kept at this temperature for 2 h. For all DRM tests, the feed gases were fixed at CH_4 = 33.33 mL/min and CO_2 = 66.67 mL/min, and the steady-state DRM activities were evaluated at different temperatures ranging from 600 °C to 800 °C under ambient pressure. For all the DRM catalytic tests, the carbon balance was close to 100% calculated from the GC results by comparing the gas composition from inlet feed and outlet products.

2.4 Data analysis

For all the DRM catalytic tests, the methane conversion (X_{CH4}) and CO_2 conversion (X_{CO2}) were calculated according to Eq. 1 and Eq. 2, respectively.

$$X_{CH4} = \frac{F_{CH4,\,in} - F_{CH4,out}}{F_{CH4,\,in}} \quad (1)$$

$$X_{CO2} = \frac{F_{CO2,\,in} - F_{CO2,out}}{F_{CO2,\,in}} \quad (2)$$

where $F_{CH4,in}$ and $F_{CH4,out}$ are the methane flow rates in the feed and in the product stream, respectively. $F_{CO2,in}$ and $F_{CO2,out}$ are the CO_2 flow rates in the feed and in the product stream, respectively. Equilibrium conversions at a given temperature was calculated by minimization of the Gibbs energy of the system.

As in previous studies [5, 14, 32], the energy evaluation of the Joule-heated system was conducted. For each catalytic test, the input voltage (*V*) and current (*I*) were recorded for both the internal Joule heating and external oven heating runs. Therefore, the input power (*P*) and the resistance (*R*) of the electrical circuit were calculated according to Eq. 3 and Eq. 4, respectively.

$$\mathrm{P} = \mathrm{VI} \tag{3}$$

$$\mathrm{R} = \frac{\mathrm{V}}{\mathrm{I}} \tag{4}$$

In order to evaluate the amount of energy consumed by the DRM reaction, the reaction heat duty (*Q*) was calculated according to the following equation:

$$\mathrm{Q} = \dot{\mathrm{H}}_{\mathrm{out}} - \dot{\mathrm{H}}_{\mathrm{in}} \tag{5}$$

where $\dot{H}_{in}$ and $\dot{H}_{out}$ are the enthalpy flows of the gas mixtures at inlet and outlet of the reactor, respectively. In this regard, the power loss (P_{loss}) of the system can be calculated according to Eq. (6):

$$\mathrm{P}_{\mathrm{loss}} = \mathrm{P} - \mathrm{Q} \tag{6}$$

The reaction heat (*Q*) can be divided into reaction chemistry heat (Q_c) and reaction sensible heat (Q_s). The reaction chemistry heat (Q_c) at 298 K was evaluated according to:

$$\mathrm{Q_c} = \sum_{\mathrm{i}} \lambda_{\mathrm{i}} \Delta \mathrm{H}_{\mathrm{i}}^{\mathrm{R}} \tag{7}$$

where ΔH_i^R is the heat of reaction at 298 K. In this regard, the reaction sensible heat (Q_s) could be evaluated according to:

$$Q_s = Q - Q_c \tag{8}$$

Finally, the theoretical specific energy demand (SE_{syn}) for syngas production during Joule-heated DRM tests was evaluated considering an energy efficiency of 95% and a recovery of 90% sensible heat [5], according to Eq. (9):

$$SE_{syn} = \frac{Q_r + 0.1 * Q_s}{0.95 * (\mathrm{F_{CO2,\,in}} - \mathrm{F_{CO2,out}})} \tag{9}$$

3. Results and discussion

3.1 SiSiC foam and catalyst characterization

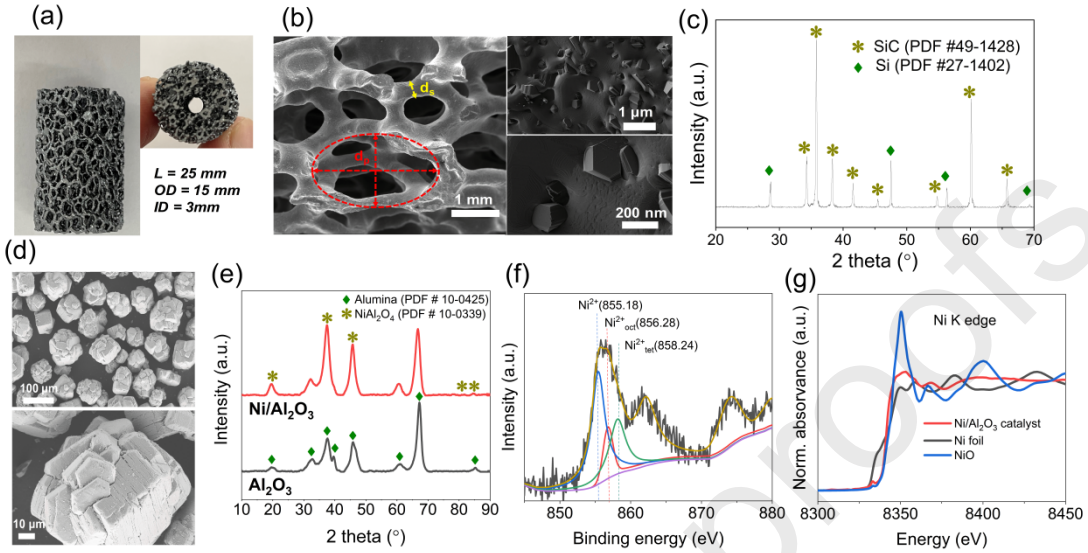

Figure 1. Characterization results of the Joule heating element (SiSiC foam) and DRM catalyst (Ni/Al_2O_3) applied in the present work. (a) Front (left) and top (right) views of the SiSiC foam; (b) SEM images of the SiSiC foam with a representative description of d_p and d_s measurements; (c) X-ray diffraction patten of the SiSiC foam; (d) SEM images of the Ni/Al_2O_3 DRM catalyst adopted in this work; (e) X-ray diffraction pattens of the Al_2O_3 support and Ni/Al_2O_3 catalyst; (f) XPS results of the Ni/Al_2O_3 catalyst; and (g) normalized X-ray absorption near edge structure (XANES) spectra of the Ni/Al_2O_3 catalyst as well as the reference Ni foil and NiO samples.

Prior the catalytic tests, the selected Joule heating element, *i.e.*, SiSiC foam, and DRM catalyst, *i.e.*, Ni/Al_2O_3, were systematically characterized to gain a comprehensive understanding of their properties. Figure 1(a) shows the front (left) and top (right) views of the adopted SiSiC foam in present work. The cylindrical hole (3 mm) positioned along the centerline position of the foam allows for the placement of a sliding thermocouple (T_c) for temperature distribution measurements. As shown in Figure 1(b), the foam with porous structure (25 PPI) exhibited an average pore dimeter of 2.29 mm and a strut dimeter of 0.46 mm (Table 1). A total foam porosity of 0.73 was estimated by ethanol picometry method (Table 1). The porous structure of the foam may facilitate the packing of pellet catalysts, creating a packed bed with intimate contact between the catalyst and the heating element, and this arrangement may ensure excellent heat transfer properties, while the tortuous gas flow path enhances the mass transfer rates [38]. Upon zooming in the SEM images, we could clearly observe the Si particles infiltrated on the SiC surface (Figure

1(b)), in line with the XRD results (Figure 1(c)), which evident the presence of both Si phase (PDF #27-1402) and SiC phase (PDF #49-1428) [14, 40]. This infiltrated Si is able to modify the electrical resistance and enhance the chemical stability of the bulk SiC material [40, 41]. Figure S1 shows SEM images of the SiSiC foam with broken surfaces.

Table 1. Geometrical and phase properties of the adopted SiSiC foam in this study.

OD (mm)	ID (mm)	L (mm)	PPI	Porosity (%)	d_s (mm)	d_p (mm)	Phase composition
15	3	25	25	73	0.46	2.29	Si / SiC

As shown in Figure 1(d), the prepared Ni/Al_2O_3 catalyst features a laminated cubic structure with an average size of approx. 80 µm. The impregnation of Ni onto the Al_2O_3 support (Figure S2) does not significantly alter the support size but creates additional pores with the specific surface area increased from 76 m^2/g to 81 m^2/g (Table S1 and Figure S3). This is accompanied by the formation of the $NiAl_2O_4$ phase, as indicated by the XRD data (Figure 1(e)). It has been reported that the formation of $NiAl_2O_4$ phase with strong metal-support interaction is beneficial to stabilize Ni particles by preventing sintering at elevated reaction temperatures [42].

As shown in Figure 1(f), the XPS spectrum of the Ni/Al_2O_3 sample can be deconvolved into three peaks. The peak at binding energy of 855.18 eV corresponds to the P1 peak of Ni 2p, while the peaks at 856.28 eV and 858.24 eV represent the P2 peaks of Ni 2p, indicating Ni^{2+} in octahedral and tetrahedral coordination sites, respectively. The results obtained are consistent with previous literature reports and suggest a good interaction between Ni and Al_2O_3 support [43, 44]. The Ni K-edge XAS spectrum collected for the Ni/Al_2O_3 sample is depicted alongside the reference spectra of Ni foil and NiO samples in Figure 1(g). The pre-edge peak of the Ni/Al_2O_3 sample resembles that of the NiO (Ni^{2+}) reference and is assigned to the dipole-forbidden but quadrupole-allowed transition (1s to 3d) [45]. The increases in the pre-edge peak intensity of Ni/Al_2O_3 sample indicating a strong interaction between the support and Ni species, as suggested by previous works [45, 46]. The white line intensity of Ni/Al_2O_3 sample is higher that of the Ni foil reference, consistent with the presence of a small portion of oxidized Ni species [47].

In short, we have characterized the selected materials in this section,

including the heating element, *i.e.*, SiSiC open-cell foam, and the DRM catalyst, *i.e.*, Ni/Al_2O_3 sample. The results indicate that we have a heating substrate with an appropriate composition and structure for Joule heating and for packing the pellet catalysts. The prepared Ni/Al_2O_3 demonstrates reasonable composition and properties for the dry reforming of methane reaction. This enables us to explore the benefits of direct internal Joule heating of SiSiC open-cell foam packed with Ni-based catalysts for an electrified dry reforming of methane process.

3.2 Joule heating of the bare SiSiC foam in N_2

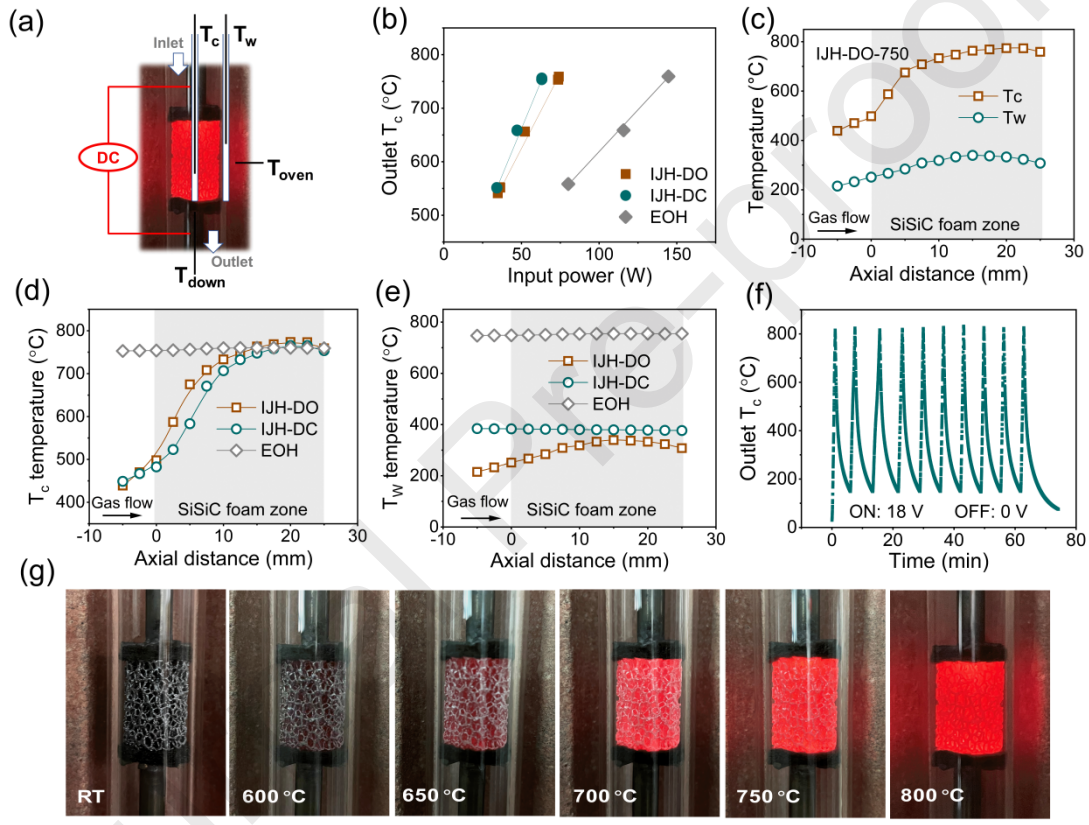

Figure 2. Joule heating of the bare SiSiC open-cell foam in flowing N_2. (a) Schematic representation of temperature measurements in the Joule-heated reactor system, T_c and T_w were measured from sliding thermocouples located at the centerline of the foam and the outer wall of the quartz reactor tube, respectively, T_{down} was measured at the downstream of the foam at centerline position and the T_{oven} was measured at the oven inner wall at the mid of the reactor position; (b) outlet T_c temperature as a function of input power in different heating modes including IJH-DO, IJH-DC and EOH; (c) T_c and T_w temperature distribution profiles from IJH-DO-750; comparison of (d) T_c and (e) T_w temperature distribution profiles from different heating modes at fixed outlet T_c of 750 °C; (f) rapid Joule heating temperature response with fast input power on and off; (g) SiSiC foam images during Joule heating from room

temperature (RT) to 800 °C. All tests in this section were carried out with a bare SiSiC foam (without catalyst packing) in a 100 mL/min N_2 flow at ambient pressure.

Before conducting the DRM catalytic tests, we systematically evaluated the Joule heating properties of the investigated system by direct internally heating a bare SiSiC foam in an inert nitrogen atmosphere (100 mL/min N_2). Monitoring the temperatures along the reactor is crucial during the Joule heating process. To achieve this, we have placed several thermocouples, as shown in Figure 2(a), at dedicated locations within the reactor. This includes two sliding thermocouples, T_c and T_w, for measuring the temperature distribution from the foam centerline and the reactor outer wall, respectively, while T_{down} for the downstream temperature after the foam and T_{oven} for monitoring and controlling the oven temperature.

As shown in Figure 2(b), the SiSiC foam can be heated by both the Joule effect (direct heating) and an external oven (indirect heating) to high temperatures relevant for the DRM reaction. The outlet T_c temperature, measured at the bottom of the foam, demonstrated a linear correlation with input power, regardless of the heating mode, in line with previous reports [5, 14, 32]. Notably, a higher input power is necessary to achieve the same outlet T_c temperature when using external oven heating compared to direct internal Joule heating. For instance, 144 W was required for external oven heating to reach outlet T_c of 750 °C, whereas only 73 W and 61 W were needed for Joule heating with the oven door open and closed, respectively. During direct internal Joule heating, both T_c and T_w show increasing temperature profiles along the foam region in gas flow direction, as shown by IJH-DO-750 in Figure 2(c). Notably, the foam centerline temperature T_c was significantly higher, by 200-400 °C, than the reactor outer wall temperature T_w at the same axial position. The temperature difference between T_c and T_w does not accurately represent the radial temperature distribution within the foam. Although the outer surface temperature of the foam was not directly measured, it is expected to be significantly higher than T_w. Despite the presence of heat dissipation, the volumetric nature of Joule heating is likely to result in a relatively uniform radial temperature distribution within the foam. The rising temperature profile indicates that when designing the Joule-heated endothermic DRM process, it is essential to avoid packing the catalyst in the foam inlet region, where temperatures are low and not favorable for catalyst. Instead, the inlet section can be utilized for feed gas preheating.

By comparing Figure 2(d) and Figure 2(e), it is evident that to reach the same outlet T_c of 750 °C, the T_w remains constant along the foam region during external oven heating, while significantly lower T_w temperatures were observed with internal Joule heating. The same trend is noted for other outlet

T_c temperatures of 700 °C and 650 °C (Figure S4). This suggests that external oven heating necessitates heating a larger area to reach the target foam temperature, making it more energy-consuming compared to internal Joule heating, which, however, is able to selectively heat only the SiSiC foam, consistent with the lower input power requirements shown in Figure 2(b). The selective Joule heating of only the target internal structures may have other potential advantages, such as avoiding undesired gas-phase side reactions [48]. For internal Joule heating modes, T_w is lower in the oven door open condition (IJH-DO) compared to the closed condition (IJH-DC) due to increased thermal loss to the surroundings (Figure 2(e)). Consequently, a bit higher T_c temperature was observed along the axial position (Figure 2(d)), indicates the requirement of a higher input power. This is consistent with the results shown in Figure 2(b).

Direct internal Joule heating of the SiSiC open-cell foam demonstrates the potential for rapid heating and cooling cycles. As illustrated in Figure 2(f), by periodically turning on (18 V) and off (0 V) the power generator, the system can quickly control temperatures between 150 °C and 800 °C. This capability may allow for the rapid startup and shutdown of the endothermic reactions, enabling the system to operate with a fast temperature response that can adapt to the intermittent nature of renewable energy sources [9, 26, 49]. Figure 2(g) displays the images of SiSiC foam at different Joule heating temperatures up to 800 °C. This provides clear evidence that Joule heating of the foam delivers selective, uniform, and stable heating, which are the key advantages of direct volumetric internal heating that worth a further exploration in efficient driving the endothermic dry reforming of methane reaction.

3.3 Joule-heated DRM performance

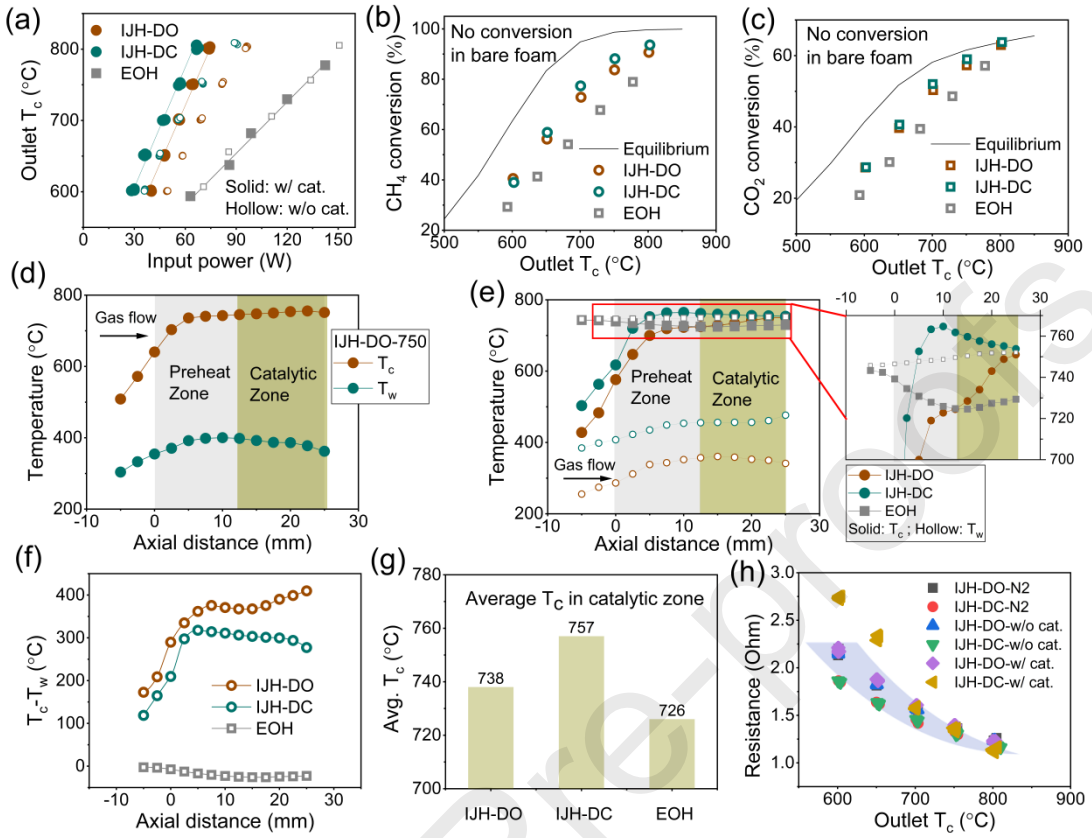

Figure 3. Joule-heated dry reforming of methane results. (a) Measured outlet T_c temperature as a function of input power from different heating modes with and without the presence of Ni/Al_2O_3 catalyst in DRM feed; (b) CH_4 conversion and (c) CO_2 conversion as a function of outlet T_c temperature from different heating modes in Joule-heated DRM tests; (d) T_c and T_w temperature distribution profiles from IJH-DO-750; (e) comparison of temperature profiles from different heating modes at fixed outlet T_c temperature of 750 °C; (f) comparison of T_c-T_w profiles and (g) average T_c from different heating mode at fixed outlet T_c temperature of 750 °C; (h) calculated electrical resistance as a function of outlet T_c temperature from all the Joule-heated runs. All tests in this section were carried out with CH_4 = 33.33 mL/min, CO_2 = 66.67 mL/min; in the case of Joule-heated DRM runs, the packed catalyst loading was 100 mg Ni/Al_2O_3 diluted in 3 g quartz sand.

To evaluate the DRM catalytic performance, 100 mg pellet Ni/Al_2O_3 catalysts were diluted in 3 g quartz sand and packed in the voids of the SiSiC foam. The packed catalytic bed filled only half of the foam volume, with the upper unfilled half serving as a preheater, as suggested from the rising T profiles in Figure 2(c). All DRM tests in this section were carried out in CH_4 = 33.33 mL/min, CO_2 = 66.67 mL/min, at ambient pressure. It is important to note that in the experimental campaign, the target system temperature was regulated

by the outlet T_c temperature during internal Joule heating, and by the T_{oven} temperature during external oven heating.

As shown in Figure 3(a), the outlet T_c exhibited as well a linear correlation with input power in DRM feed, regardless of the catalyst presence and the heating mode, similar to the results obtained from Joule heating of only the bare foam in N_2 (Figure 2(b)). It requires significantly less input power for internal Joule heating to reach same outlet T_c temperature, as compared to external oven heating, thanks to the selective internal Joule heating, in line with the results obtained from Figure 2. For example, only 65 W for internal Joule heating (IJH-DC) to reach 800 °C compared to 143 W for external oven heating. The Joule-heated processes displayed the same heating slope in open and closed oven conditions, indicates a similar heat dissipation process, however, in contrast to oven heating, which exhibited a steeper heating slope. The heating curves are overlapped for external oven heating with and without the presence of catalyst. However, in the cases of internal Joule heating, less input power was required when the catalyst present, this can be attributed to the use of a thin layer of quartz wool covering the gap between the foam and the quartz tube reactor, which acts as a thermal insulation layer. In contrast, no quartz wool was used in the bare foam configuration.

It is important to mention that the bare foam (without catalyst packing) was tested with DRM feed, where hardly any methane or CO_2 conversions could be observed at temperatures up to 800 °C, indicating that the bare foam is inert with respect to the DRM reaction. With the presence of Ni/Al_2O_3 catalyst, Figure 3(b) and (c) show the methane conversion and CO_2 conversion as a function of outlet T_c temperature, respectively. Outlet T_c was selected as the representative reference temperature to compare the obtained conversions with equilibrium conversions, as suggest by Balzarotti and coworkers [50]. It should be noted that for oven heating, the conversion results were plotted based on the measured outlet T_c temperatures instead of the target T_{oven} temperatures. For all the tests, the conversions were lower than that of equilibrium, indicating that the DRM runs were operated in kinetic controlled regime. Interestingly, even under the same feed conditions, the internal Joule heating processes exhibited superior DRM activities, achieving higher methane and CO_2 conversions compared to external oven heating. Among them, the IJH-DC configuration exhibited the best performance, with the highest methane conversion of 94% and CO_2 conversion of 64% achieved at outlet T_c of 800 °C. However, the EOH mode demonstrated approx. 10% lower methane conversion and about 5% lower CO_2 conversion compared to that of IJH-DC configuration even at same outlet T_c temperatures. The results for methane and CO_2 conversions as a function of input power are shown in Figure S5 to illustrate the input-output relationship. It is important to note that

stable conversions and a carbon balance close to 100% were achieved throughout the tests, with no carbon deposits observed after unloading the reactor. Table S2 compares the results of this study with literature reports on Joule-heated dry reforming of methane. This work represents the first report on Joule-heated DRM using a packed bed configuration and demonstrates excellent DRM activity achieved with non-noble Ni-based catalysts.

The dry reforming of methane reaction is highly dependent on reaction temperature. In present work, the same Ni-based catalysts were used for both external oven heating and internal Joule heating, the DRM activity is expected to be identical at the same temperature. To explain the differences observed in Figure 3(b) and (c), a detailed analysis of the temperature distribution was conducted to evaluate the advantages of direct internal Joule heating compared to indirect external oven heating. As an example, Figure 3(d) shows the T_c and T_w temperature profiles of IJH-DC-750 along the axial direction, while the results for other temperatures can be found in Figure S6. A T_c temperature of 570 °C was measured at the top of the foam, which went through a preheating process in the upper half foam to reach 723 °C before entering the catalytic bed (Figure 3(d)). Despite the proceeding of endothermic DRM reaction, the temperature displayed a gradual increase and ultimately reaching the target of 750 °C at the end of the catalytic bed. The T_w temperature exhibits an increasing trend during the preheating process followed by a slightly decrease in the endothermic catalytic region. T_w remains significantly lower than T_c throughout the reactor, indicating the selective properties of internal Joule heating, which ensures an energy-saving process ((Figure 3(a)). However, T_w does not accurately reflect the radial temperature distribution within the foam. We assume that the foam has uniform temperature distribution in radial position to the outer wall due to the effects of volumetric Joule heating and the fact that the catalysts is in close contact with the heating sources, even though a small amount of thermal dissipation may occur.

Figure 3(e) compares the T_c and T_w temperature distribution profiles from the three different heating modes at same outlet T_c of 750 °C. It is evident that T_w exhibits distinctly different profiles, remaining almost constant at 800 °C for EOH, while being significantly lower for the IJH cases, particularly in the oven door open condition where more heat dissipation is expected (Figure 3(e)). Figure 3(f) displays the calculated radial temperature difference between T_c and T_w along the axial coordinate. Compared to conventional external oven heating, the direct internal Joule heating selectively heats only the catalytic bed, resulting in a reactor wall temperature (T_w) can be at least 300 °C lower than the foam centerline temperature (T_c) in the foam region, leading to a significant reduction of reactor material requirements and costs. In the case of

external oven heating, where heat is supplied from outside the reactor, a decreasing T_c profile with temperature as low as approx. 725 °C observed (Figure 3(e)). Given the fact that SiSiC foam is a thermally conductive internal structure that enhances heat transfer [51], we can expect that T_c would be even lower if the SiSiC foam were absent [50]. In contrast, a rising T_c temperature profile was noticed for IJH-DO across the catalytic bed until reaching the target outlet temperature. With improved thermal insulation, a rapid increase in T_c was noted for IJH-DC in the first part of the foam, achieving a maximum temperature of 765 °C. Subsequently, T_c gradually decreased with the proceeding of the endothermic DRM reaction, arriving the target outlet temperature of 750 °C. As a result, a higher average T_c temperature of 757 °C was achieved in the reaction zone for IJH-DC (Figure 3(g)), followed by 738 °C and 726 °C for IJH-DO and EOH, respectively. This explains that DRM active follows the sequence of IJH-DC > IJH-DO > EOH, suggested by Figure 3(b) and (c). The average T_c temperatures were calculated for other operation conditions and displaced a similar trend (Figure S7). Furthermore, no cold spots were observed across the catalytic bed during direct internal Joule heating, this presents a significant advantage over external oven heating to avoid carbon deposition associated with catalyst deactivation [52, 53].

The contact between the SiSiC foam and the electrodes is a critical factor influencing the stability and efficiency of the Joule-heated system. Insufficient contact can result in significant contact resistance, leading to localized high temperatures. Furthermore, the thermal expansion of the SiSiC foam during heating and cooling cycles may cause a loss of electrical contact. In this work, a robust metallic frame structure was adopted to fix the electrodes, in order to ensure optimal foam-electrode contact. As shown in Figure 3(h), we have summarized the calculated electrical resistance from all the Joule heating tests carried out in this work, and plotted as a function of outlet T_c temperature. The electrical resistance exhibited a decreasing trend with rising outlet T_c temperature, in line with simi-conductor nature of SiC material [54], as well as the previous reports [5, 14, 32]. The electrical resistance may vary at lower temperatures due to imperfect contact between the foam and the electrodes. However, thanks to the thermal expansion at high temperatures which may result in improved electric contact, the electrical resistances were almost superimposed at temperatures above 700 °C, proving the reproducibility of the system with stable Joule heating performance, even under DRM reaction conditions.

3.4 Energy evaluation of the Joule-heated DRM processes

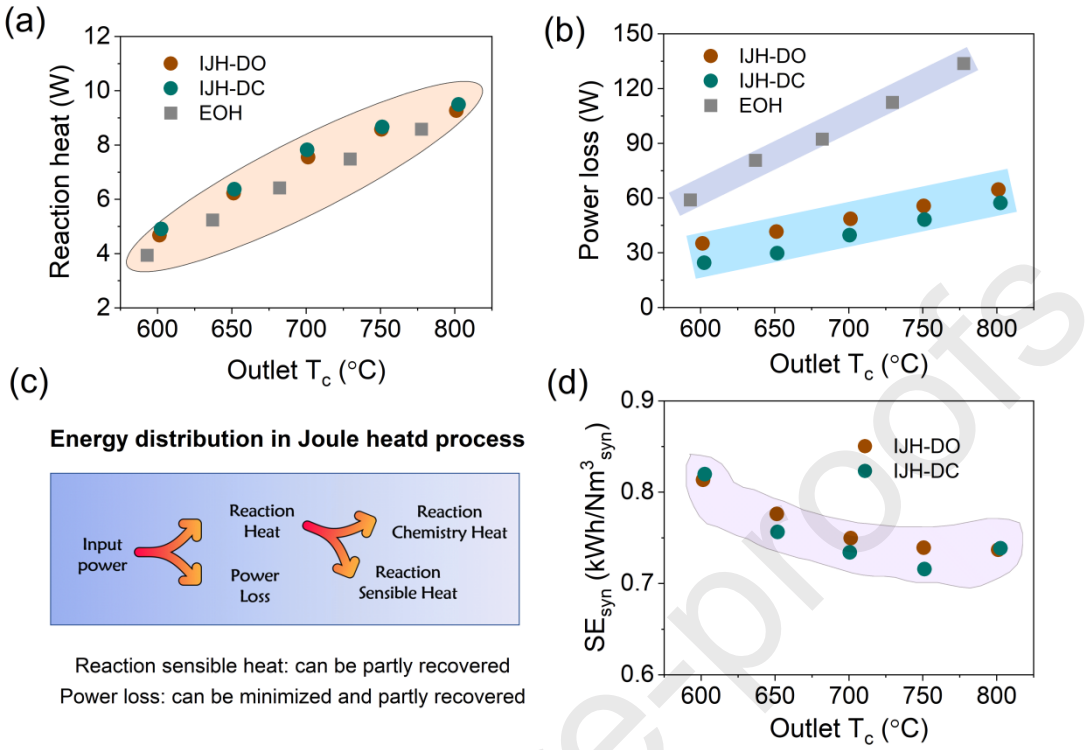

Figure 4. Energy analysis of the Joule-heated dry reforming of methane runs. (a) Reaction heat and (b) power loss and as a function of outlet T_c temperature from different heating modes; (c) energy flow of the Joule-heated catalytic process; (d) specific energy demand for syngas production (SE_{syn}) as a function of outlet T_c from different heating modes. SE_{syn} was calculated considering an energy efficiency of 95% and a recovery of 90% sensible heat.

As an innovative method to supply the required heat for endothermic reaction, it is important to assess the energy distribution of the Joule-heated DRM process. The required reaction heat for the DRM process under different heating modes was calculated and presented in Figure 4(a). The reaction heat ranges from 4 to 10 W, showing an increasing trend with rising temperature. Moreover, it demonstrates that more energy was used as reaction heat at the same outlet T_c temperature in the IJH-DC mode, followed by the IJH-DO and EOH, consistent with the previously reported DRM activity in Figure 3(b) and (c). The power loss of the system, calculated by subtracting the required reaction heat from the input power, is illustrated in Figure 4b and shows a linear correlation with the outlet T_c temperature, regardless of the heating mode. This aligns with previous reports and indicates that thermal dissipation through natural convection is the primary energy loss of the system [5, 14, 32]. The IJH modes displayed similar power loss characteristics whether the oven door was open or closed, differing from external oven heating, consistent

with the results presented in Figure 2(b) and Figure 3(a).

As shown in Figure 4(c), in a typical electrified catalytic process, a portion of the input power is dedicated to driving the reaction, *i.e.*, reaction heat, while the rest is lost through heat dissipation at high temperatures. This power loss can be minimized through better thermal insulation or improved reactor design [9, 55], moreover, some of such thermal energy loss can be partially recovered through heat exchange. Only a fraction of the energy from the reaction heat is necessary to drive the reaction itself, *i.e.*, reaction chemistry heat, with the rest part used to heat the gases to target reaction temperatures, *i.e.*, reaction sensible heat. The reaction sensible heat is in principle can also be captured as thermal energy via heat exchange [5, 56]. The detailed energy distribution results from different heating modes are presented in Table S3. In this context, a specific energy demand for syngas production (SE_{syn}) was calculated during eDRM considering an energy efficiency of 95% and a recovery of 90% sensible heat [5], and the results are presented in Figure 4(d). Compared to the open oven door condition, the IJH-DC mode exhibited a slightly lower SE_{syn} at the same outlet T_c temperature, which can be attribute to the enhanced DRM activity observed (Figure 3(b) and (c)). The lowest SE_{syn} of 0.71 kWh/Nm^3_{syn} was achieved during the IJH-DC-750 process. Such results are very attractive and in principle can be achieved by optimizing the process design. The H_2/CO ratio of produced syngas in the present work falls in the range of 0.46-0.52 (Figure S8(a)), due to the fact that a higher stoichiometric feed ratio (CO_2/CH_4 = 2) was used, which facilitates a significant reverse water-gas shift reaction, as suggested by the calculated net CO_2 consumption per converted reactant CH_4 in Figure S8(b).

3.5 Discussion

Alongside the environmental benefits and the potential to store intermittent renewable energy in the form of chemicals [6, 9], the transition from fuel combustion heating to process electrification via Joule heating based on renewable energy offers substantial advantages for driving endothermic catalytic reactions [9, 20]. As a novel and advanced method, it requires dedicated reactor engineering to effectively maximize the benefits of Joule heating in driving endothermic reactions. Indeed, the direct Joule heating of SiSiC open-cell foams has been investigated with a Rh/Al_2O_3 catalyst washcoated configuration [5, 14, 32]. As an extension, this work presents a catalyst packed bed configuration where non-noble metal Ni-based pellet catalysts were placed within the voids of the SiSiC open-cell foam for dry reforming of methane. Moreover, the introducing of dedicated thermocouples for temperature distribution measurement allows for a clear understanding of the advantages of direct internal Joule heating, compared to the conventional

external oven heating.

So far, most studies reported for Joule-heated processes are based on catalyst washcoat configuration [13, 14, 16-18, 34, 36, 37, 49, 57-59]. The washcoat configuration offers excellent heat transfer properties as the catalyst can be located in direct contact with the heating source, however, on the other hand, it might suffer from limited catalyst coating strength, result in mass loss and diminished catalytic activity, especially under high gas velocity conditions. In this work, the porous structure of open-cell foam enables a packed configuration with superior heat transfer properties, while avoid potential mechanical adhesion issues associated with washcoating. However, when scaling up this catalyst packed open-cell foam configuration, it is crucial to consider the possible issues associated with pressure drop and effective packing volume.

Moving from external heating to direct internal heating within the reactor, the Joule-heated reactor configuration allows for selective heating of only the target elements. Once the target reaction temperature is reached, the wall temperature (T_w) can be significantly lower than the temperature in the catalytic bed (T_c), as illustrated in Figure 3(d). Moreover, the T_{down} which was measured 2 mm below the foam exhibited approx. 100°C lower temperatures than the outlet T_c. This may offer several advantages: (i) improved energy efficiency, as energy can be precisely used in where reaction is needed, rather than in the surrounding environment, as demonstrated in Figure 3(a); (ii) reduced reactor material costs, as selective heating generates the highest temperatures within the catalytic bed while substantially lowering the reactor wall temperature, as shown in Figure 3(d), this reduction in wall temperature decreases material requirements, leading to substantial cost savings, which is a critical consideration in large-scale reforming applications; (iii) the potential to inhibit unwanted gas phase reactions, such as oxidative dehydrogenation reactions suggested by Ramirez and coworkers [48], and methane pyrolysis *etc.*, where high temperature undesired homogeneous reactions may lead to low selectivity of target products. This advantage can be further explored in the future.

The SiSiC open-cell foam, with its porous structure, its direct Joule heating ensures volumetric heating and promotes a uniform temperature distribution within the reactor, leveraging the excellent heat transfer properties of SiSiC material [51, 54]. This uniform heating helps prevent the cold spots formation that commonly associated with external heating, therefore avoid possible carbon deposition that may lead to catalyst deactivation [2, 52]. Additionally, this volumetric and uniform heating can achieve higher average temperatures in the catalytic bed, resulting in an increased catalytic activity compared to

external oven heating, as evident by Figure 3(b) and (c).

The Joule effect enables the complete transformation of electric energy into thermal energy [9, 60]. In this work, a quartz tube reactor was utilized in order to facilitate the observation of experimental phenomena, however, a large amount of heat was dissipated due to inadequate thermal insulation. In principle, a stainless-steel tube reactor can be designed with improved thermal insulation, and by operating under intensified conditions, it is possible to significantly improve process energy efficiency [28, 32]. Furthermore, a stainless-steel tube reactor enables the reforming reaction to be conducted under pressurized conditions [32]. However, the stainless-steel tube reactor should be carefully designed to avoid possible electric issues, this can be achieved for example by placing an electric insulation layer between the Joule heating element and the stainless-steel tube [5, 14, 32].

4. Conclusions

In this study, we have investigated the direct internal Joule heating of a silicon infiltrated silicon carbide (SiSiC) open-cell foam packed with non-noble metal Ni-based pellet catalysts for dry reforming of methane. The interconnected porous structure of SiSiC foam serves as an effective Joule heating substrate, enabling selective and volumetric heating of the pellet catalysts located within the foam voids. Several dedicated thermocouples were strategically placed within the catalytic bed to ensure precise monitoring and evaluation of the internal Joule heating process. Compared to conventional external oven heating, the direct internal Joule heating selectively heated only the catalytic bed, resulting in a reactor wall temperature (T_w) can be approx. 300 °C lower than the foam centerline temperature (T_c), leading to a significant reduction of reactor material requirements and costs. Additionally, the selective heating requires considerably lower input power, only 65 W (IJH-DC) to reach 800 °C compared to 143 W for external oven heating. Furthermore, the porous structure of SiSiC foam facilitates volumetric heating of the catalytic bed, resulting in a more uniform temperature distribution (T_c) without cold spots noticed. Such uniform heating contributes to an average T_c temperature in the catalytic bed that is approx. 30 °C higher than that from external oven heating. The improved temperature distribution leads to promoted dry reforming of methane (DRM) activities, with methane conversion of 94% and CO_2 conversion of 64% achieved at outlet T_c of 800 °C, which are approx. 10% higher in methane conversion and 5% higher in CO_2 conversion compared to external oven heating under the same outlet foam temperatures. The Joule heating process ensures a significantly low specific energy demand for

syngas production, with approx. 0.71 kWh/Nm³ achieved in a simulated process. In addition to the general benefits of decarbonization and the potential to store intermittent renewable energy, this work demonstrates that the transition from external heating to direct internal Joule heating provides several advantages to enhance the dry reforming of methane reaction, and the insights obtained in the present work are in principle applicable to other endothermic reactions.

Acknowledgments

The authors gratefully acknowledge the support of this work from Chinese Academy of Sciences (CAS) and Shanghai Advanced Research Institute (SARI). We thank Shuqing Li (SARI) and Bingrong Pan (SARI) for their technical support with respect to catalysts tests, and Changkun Yuan (SARI) is acknowledged for SEM measurements. We could like to thank Shanghai Synchrotron Radiation Facility for providing beamtime at BL11B beamline, and acknowledge in particular Dr. Tao Gan (SARI) for his technical support during XAS experiments.

References

[1] M. Usman, W.W. Daud, H.F. Abbas, Dry reforming of methane: Influence of process parameters - A review, Renewable and Sustainable Energy Reviews, 45 (2015) 710-744.

[2] J.-M. Lavoie, Review on dry reforming of methane, a potentially more environmentally-friendly approach to the increasing natural gas exploitation, Frontiers in Chemistry, 2 (2014) 81.

[3] Y. Song, E. Ozdemir, S. Ramesh, A. Adishev, S. Subramanian, A. Harale, M. Albuali, B.A. Fadhel, A. Jamal, D. Moon, Dry reforming of methane by stable Ni-Mo nanocatalysts on single-crystalline MgO, Science, 367 (2020) 777-781.

[4] L.C. Buelens, V.V. Galvita, H. Poelman, C. Detavernier, G.B. Marin, Super-dry reforming of methane intensifies CO_2 utilization via Le Chatelier's principle, Science, 354 (2016) 449-452.

[5] L. Zheng, M. Ambrosetti, A. Beretta, G. Groppi, E. Tronconi, Electrified CO_2 valorization driven by direct Joule heating of catalytic cellular substrates,

Chemical Engineering Journal, 466 (2023) 143154.

[6] G.P. Thiel, A.K. Stark, To decarbonize industry, we must decarbonize heat, Joule, 5 (2021) 531.

[7] K.M. Van Geem, V.V. Galvita, G.B. Marin, Making chemicals with electricity, Science, 364 (2019) 734.

[8] D.S. Mallapragada, Y. Dvorkin, M.A. Modestino, D.V. Esposito, W.A. Smith, B.-M. Hodge, M.P. Harold, V.M. Donnelly, A. Nuz, C. Bloomquist, K. Baker, L.C. Grabow, Y. Yan, N.N. Rajput, R.L. Hartman, E.J. Biddinger, E.S. Aydil, A.D. Taylor, Decarbonization of the chemical industry through electrification: Barriers and opportunities, Joule, 7 (2023) 23.

[9] L. Zheng, M. Ambrosetti, E. Tronconi, Joule-heated catalytic reactors toward decarbonization and process intensification: A review, ACS Engineering Au, 4 (2023) 4.

[10] V. Palma, D. Barba, M. Cortese, M. Martino, S. Renda, E. Meloni, Microwaves and heterogeneous catalysis: A review on selected catalytic processes, Catalysts, 10 (2020) 246.

[11] D.G. Kang, K. Sung, H. Yong, K. Jeong, M. Choi, H.-T. Kim, S. Kwon, S.M. Kim, J.S. Myung, D.W. Kim, J.H. Park, J.W. Han, S.-J. Kim, Electrified inductive heating for sustainable utilization of liquid hydrogenated organics, Joule, 8 (2024) 2374.

[12] C.H. Lin, C. Wan, Z. Ru, C. Cremers, P. Mohapatra, D.L. Mantle, K. Tamakuwala, A.B. Höfelmann, M.W. Kanan, J. Rivas-Davila, J.A. Fan, Electrified thermochemical reaction systems with high-frequency metamaterial reactors, Joule, (2024) DOI: 10.1016/j.joule.2024.1007.1017.

[13] S.T. Wismann, J.S. Engbæk, S.B. Vendelbo, F.B. Bendixen, W.L. Eriksen, K. Aasberg-Petersen, C. Frandsen, I. Chorkendorff, P.M. Mortensen, Electrified methane reforming: A compact approach to greener industrial hydrogen production, Science, 364 (2019) 756.

[14] L. Zheng, M. Ambrosetti, D. Marangoni, A. Beretta, G. Groppi, E. Tronconi, Electrified methane steam reforming on a washcoated SiSiC foam for low-carbon hydrogen production, AIChE Journal, 69 (2023) e17620.

[15] Q. Dong, A.D. Lele, X. Zhao, S. Li, S. Cheng, Y. Wang, M. Cui, M. Guo, A.H. Brozena, Y. Lin, Depolymerization of plastics by means of electrified spatiotemporal heating, Nature, 616 (2023) 488.

[16] Q. Dong, Y. Yao, S. Cheng, K. Alexopoulos, J. Gao, S. Srinivas, Y. Wang, Y. Pei, C. Zheng, A.H. Brozena, Programmable heating and quenching for efficient thermochemical synthesis, Nature, 605 (2022) 470.

[17] K. Yu, C. Wang, W. Zheng, D.G. Vlachos, Dynamic electrification of dry reforming of methane with *in situ* catalyst regeneration, ACS Energy Letters, 8 (2023) 1050.

[18] Q. Ma, Y. Gao, B. Sun, J. Du, H. Zhang, D. Ma, Grave-to-cradle dry reforming of plastics via Joule heating, Nature Communications, 15 (2024) 8243.

[19] X. Mei, X. Zhu, Y. Zhang, Z. Zhang, Z. Zhong, Y. Xin, J. Zhang, Decreasing the catalytic ignition temperature of diesel soot using electrified conductive oxide catalysts, Nature Catalysis, 4 (2021) 1002.

[20] M. Idamakanti, E.B. Ledesma, R.R. Ratnakar, M.P. Harold, V. Balakotaiah, P. Bollini, Electrified catalysts for endothermic chemical processes: Materials needs, advances, and challenges, ACS Engineering Au, 4 (2023) 71.

[21] D. Maporti, R. Nardi, S. Guffanti, C. Vianello, P. Mocellin, G. Pauletto, Techno-economic analysis of electrified biogas reforming, Chemical Engineering Transactions, 96 (2022) 163-168.

[22] H. Song, Y. Liu, H. Bian, M. Shen, X. Lin, Energy, environment, and economic analyses on a novel hydrogen production method by electrified steam methane reforming with renewable energy accommodation, Energy Conversion and Management, 258 (2022) 115513.

[23] T.N. Do, H. Kwon, M. Park, C. Kim, Y.T. Kim, J. Kim, Carbon-neutral hydrogen production from natural gas via electrified steam reforming: Techno-economic-environmental perspective, Energy Conversion and Management, 279 (2023) 116758.

[24] D. Maporti, S. Guffanti, F. Galli, P. Mocellin, G. Pauletto, Towards sustainable hydrogen production: Integrating electrified and convective steam reforming, and carbon capture and storage, Chemical Engineering Journal, 499 (2024) 156357.

[25] Y.R. Lu, P.A. Nikrityuk, Scale-up studies on electrically driven steam methane reforming, Fuel, 319 (2022) 123596.

[26] S.T. Wismann, J.S. Engbaek, S.B. Vendelbo, W.L. Eriksen, C. Frandsen, P.M. Mortensen, I. Chorkendorff, Electrified methane reforming: Elucidating

transient phenomena, Chemical Engineering Journal, 425 (2021) 131509.

[27] S.T. Wismann, J.S. Engbæk, S.B. Vendelbo, W.L. Eriksen, C. Frandsen, P.M. Mortensen, I. Chorkendorff, Electrified methane reforming: understanding the dynamic interplay, Industrial & Engineering Chemistry Research, 58 (2019) 23380.

[28] T.N. From, B. Partoon, M. Rautenbach, M. Østberg, A. Bentien, K. Aasberg-Petersen, P.M. Mortensen, Electrified steam methane reforming of biogas for sustainable syngas manufacturing and next-generation of plant design: A pilot plant study, Chemical Engineering Journal, 479 (2024) 147205.

[29] V. Balakotaiah, R.R. Ratnakar, Modular reactors with electrical resistance heating for hydrocarbon cracking and other endothermic reactions, AIChE Journal, 68 (2022) e17542.

[30] Q. Wang, Y. Ren, H. Liu, H. Liu, X. Wang, Z. Gu, L. Zhang, Simulation and enhancement of axial temperature distribution in a reactor filled with in-situ electrically heated structured catalyst, International Journal of Hydrogen Energy, 55 (2024) 217-224.

[31] E. Selvam, K. Yu, J. Ngu, S. Najmi, D.G. Vlachos, Recycling polyolefin plastic waste at short contact times via rapid joule heating, Nature Communications, 15 (2024) 5662.

[32] L. Zheng, M. Ambrosetti, F. Zaio, A. Beretta, G. Groppi, E. Tronconi, Direct electrification of Rh/Al_2O_3 washcoated SiSiC foams for methane steam reforming: An experimental and modelling study, International Journal of Hydrogen Energy, 48 (2023) 14681.

[33] S. Renda, M. Cortese, G. Iervolino, M. Martino, E. Meloni, V. Palma, Electrically driven SiC-based structured catalysts for intensified reforming processes, Catalysis Today, 383 (2022) 31-43.

[34] Q. Wang, Y. Ren, X. Kuang, D. Zhu, P. Wang, L. Zhang, Electrically heated monolithic catalyst for in-situ hydrogen production by methanol steam reforming, International Journal of Hydrogen Energy, 48 (2023) 514.

[35] M. Ambrosetti, A perspective on power-to-heat in catalytic processes for decarbonization, Chemical Engineering and Processing - Process Intensification, 182 (2022) 109187.

[36] Y. Ren, H. Xu, Q. Wang, X. Kuang, L. Zhang, G. Li, Preparation and performance analysis of integrated electric heating hydrogen production foam catalyst, International Journal of Hydrogen Energy, 56 (2024) 699-708.

[37] A. Badakhsh, Y. Kwak, Y.-J. Lee, H. Jeong, Y. Kim, H. Sohn, S.W. Nam, C.W. Yoon, C.W. Park, Y.S. Jo, A compact catalytic foam reactor for decomposition of ammonia by the Joule-heating mechanism, Chemical Engineering Journal, 426 (2021) 130802.

[38] M. Bracconi, M. Ambrosetti, M. Maestri, G. Groppi, E. Tronconi, A fundamental investigation of gas/solid mass transfer in open-cell foams using a combined experimental and CFD approach, Chemical Engineering Journal, 352 (2018) 558-571.

[39] E. Meloni, G. Iervolino, V. Palma, Highly-efficient hydrogen production through the electrification of OB-SiC nickel structured catalyst: Methane steam reforming and ammonia cracking as case studies, International Journal of Hydrogen Energy, 65 (2024) 42.

[40] M. Pelanconi, G. Bianchi, P. Colombo, A. Ortona, Fabrication of dense SiSiC ceramics by a hybrid additive manufacturing process, Journal of the American Ceramic Society, 105 (2022) 786-793.

[41] G.N. Morscher, C. Baker, C. Smith, Electrical resistance of SiC fiber reinforced SiC/Si matrix composites at room temperature during tensile testing, International Journal of Applied Ceramic Technology, 11 (2014) 263-272.

[42] L. Zhou, L. Li, N. Wei, J. Li, J.-M. Basset, Effect of $NiAl_2O_4$ formation on Ni/Al_2O_3 stability during dry reforming of methane, ChemCatChem, 7 (2015) 2508-2516.

[43] S. Li, Y. Fu, W. Kong, B. Pan, C. Yuan, F. Cai, H. Zhu, J. Zhang, Y. Sun, Dually confined Ni nanoparticles by room-temperature degradation of AlN for dry reforming of methane, Applied Catalysis B: Environmental, 277 (2020) 118921.

[44] Y. Wang, L. Yao, Y. Wang, S. Wang, Q. Zhao, D. Mao, C. Hu, Low-temperature catalytic CO_2 dry reforming of methane on $Ni\text{-}Si/ZrO_2$ catalyst, ACS Catalysis, 8 (2018) 6495-6506.

[45] R. Ma, J. Gao, J. Kou, D.P. Dean, C.J. Breckner, K. Liang, B. Zhou, J.T. Miller, G. Zou, Insights into the nature of selective nickel sites on Ni/Al_2O_3 catalysts for propane dehydrogenation, ACS Catalysis, 12 (2022) 12607-12616.

[46] H.B. Yang, S.-F. Hung, S. Liu, K. Yuan, S. Miao, L. Zhang, X. Huang, H.-Y. Wang, W. Cai, R. Chen, J. Gao, X. Yang, W. Chen, Y. Huang, H.M. Chen, C.M. Li, T. Zhang, B. Liu, Atomically dispersed Ni(i) as the active site for

electrochemical CO_2 reduction, Nature Energy, 3 (2018) 140-147.

[47] E. Tusini, M. Casapu, A. Zimina, D.E. Doronkin, H. Störmer, L. Barthe, S. Belin, J.-D. Grunwaldt, Structural changes of Ni and Ni-Pt methane steam reforming catalysts during activation, reaction, and deactivation under dynamic reaction conditions, ACS Catalysis, 14 (2024) 7463-7477.

[48] A. Ramirez, J.L. Hueso, M. Abián, M.U. Alzueta, R. Mallada, J. Santamaria, Escaping undesired gas-phase chemistry: Microwave-driven selectivity enhancement in heterogeneous catalytic reactors, Science Advances, 5 (2019) eaau9000.

[49] L.G. Dou, C.J. Yan, L.S. Zhong, D. Zhang, J.Y. Zhang, X. Li, L.Y. Xiao, Enhancing CO_2 methanation over a metal foam structured catalyst by electric internal heating, Chemical Communications, 56 (2020) 205-208.

[50] R. Balzarotti, M. Ambrosetti, A. Beretta, G. Groppi, E. Tronconi, Investigation of packed conductive foams as a novel reactor configuration for methane steam reforming, Chemical Engineering Journal, 391 (2020) 123494.

[51] G.A. Slack, Thermal conductivity of pure and impure silicon, silicon carbide, and diamond, Journal of Applied Physics, 35 (1964) 3460-3466.

[52] S. Arora, R. Prasad, An overview on dry reforming of methane: strategies to reduce carbonaceous deactivation of catalysts, RSC Advances, 6 (2016) 108668-108688.

[53] O. Muraza, A. Galadima, A review on coke management during dry reforming of methane, International Journal of Energy Research, 39 (2015) 1196-1216.

[54] K. Pelissier, T. Chartier, J. Laurent, Silicon carbide heating elements, Ceramics International, 24 (1998) 371-377.

[55] M. Ambrosetti, A. Beretta, G. Groppi, E. Tronconi, A numerical investigation of electrically-heated methane steam reforming over structured catalysts, Frontiers in Chemical Engineering, 3 (2021).

[56] D. Wang, S. Li, L. Gao, A novel coal gasification system through thermochemical regenerative process of syngas sensible heat to enhance cold gas efficiency, ASME 2017 11th International Conference on Energy Sustainability, 2017.

[57] E.B. Ledesma, M. Idamakanti, P. Bollini, M.P. Harold, R.R. Ratnakar, Decarbonizing steam-methane reforming: Enhancing activity through Joule

heating of a Ni/ZrO_2-coated FeCrAl coil, ChemCatChem, 16 (2024) e202301110.

[58] H. Asmat, P. Paul, F. McLaren, L. Djumas, J. Bott, M.R. Hill, A. Tanksale, Electrified reformer for syngas production - Additive manufacturing of coated microchannel monolithic reactor, Applied Catalysis B: Environment and Energy, (2024) 124640.

[59] M. Rieks, R. Bellinghausen, N. Kockmann, L. Mleczko, Experimental study of methane dry reforming in an electrically heated reactor, International Journal of Hydrogen Energy, 40 (2015) 15940-15951.

[60] I. Dincer, 1.7 Energy and Exergy Efficiencies, in: I. Dincer (Ed.) Comprehensive Energy Systems, Elsevier, Oxford, 2018, pp. 265-339.

Declaration of Competing Interest

The authors declare that they have no known competing financial interests or personal relationships that could have appeared to influence the work reported in this paper.

Highlights:

- Direct internal Joule heating of a catalyst packed SiSiC foam configuration;
- Selective Joule heating is energy saving and ensures low reactor wall T;
- SiSiC foam provides volumetric heating with uniform T distribution;
- Internal Joule heating ensures higher DRM activity than external heating.